CHARACTERISATION OF SECONDARY PHASES IN AUSTENITIC STAINLESS STEELS USING THERMODYNAMIC SOFTWARE

CHARAKTERISTIKA SEKUNDÁRNYCH FÁZ V AUSTENITICKÝCH NEHRDZAVEJÚCICH OCELIACH S VYUŽITÍM TERMODYNAMICKÉHO SOFTVÉRU

Marián VACH , Mária DOMÁNKOVÁ, Peter GOGOLA, Martin KUSÝ, Jozef JANOVEC

Institute of Materials, Faculty of Materials Science and Technology, Slovak University of Technology, Bottova 23, 917 24 Trnava, Slovak Republic,
marian.vach@stuba.sk, maria.domankova@stuba.sk, peter.gogola@stuba.sk, martin.kusy@stuba.sk, jozef.janovec@stuba.sk,

Abstract:

Three austenitic steels (18Cr-8Ni, 18Cr-10Ni, 21Cr-30Ni) exploited for long-terms at temperatures between 600 and 800°C were investigated using metallography, transmission electron microscopy, selected area electron diffraction, energy dispersive x-ray spectroscopy, and scanning electron microscopy. Various combinations of Sigma, MC and $M_{23}C_6$ phases were found to co-exist with the austenitic matrix in the steels. At the grain boundaries of the 21Cr-30Ni steel, large $M_{23}C_6$ particles (up to 10 μm in length) were identified even if this carbide was not predicted to be in equilibrium at 800°C. Otherwise, good agreement between the thermodynamically predicted (ThermoCalc) and experimentally obtained results was stated.

Key words: ThermoCalc, TEM, SEM, austenitic steels, $M_{23}C_6$, MC, sigma phase

Abstrakt:

Tri austenitické ocele (18Cr-8Ni, 18Cr-10Ni, 21Cr-30Ni) dlhodobo vystavené teplotám medzi 600 a 800°C boli skúmané pomocou metalografie, transmisnej elektrónovej mikroskopie, difrakčnej analýzy, energiovo disperznej spektroskopie a rastrovacej elektrónovej mikroskopie. V austenitickej matrici skúmaných materiálov bola zistená koexistencia viacerých kombinácií sigma fázy, MC a $M_{23}C_6$. Veľké karbidické častice $M_{23}C_6$ (s dĺžkou až do 10μm) boli spozorované na hraniciach zŕn v oceli 21Cr-30Ni aj napriek tomu, že táto sekundárna fáza nebola podľa predikcií v rovnovážnom stave. V ostatných prípadoch bola dosiahnutá dobrá zhoda medzi termodynamickými predikciami (pomocou softwaru ThermoCalc) a experimentálnymi výsledkami.

Klúčové slová: ThermoCalc, TEM, SEM, austenitické ocele, M23C6, MC, sigma fáza.

1 INTRODUCTION

Austenitic stainless steels (ASS) are widely used in almost every industry. They can serve in aggressive environments at higher working temperatures because of their good mechanical properties and corrosion resistance [2-4]. Exposing them to temperatures around 600°C may lead to the formation of secondary phases. To prevent problems originating from precipitation processes, the evolution of secondary phases has to be well known. The

combination of experimental and computational approaches seems to be ideal for gaining necessary information.

Thanks to high alloying, ASS are very rich on secondary phases. The most common secondary phase is carbide $M_{23}C_6$. Its formation was observed widely in the temperature range from 550 to 950°C [5-7]. The precipitation of $M_{23}C_6$ at the grain boundaries leads often to intergranular corrosion. It is necessary therefore to stabilize ASS with elements showing higher affinity to carbon the chromium. Titanium and niobium used as stabilizing elements form intragranular MC carbides and contribute in this way to bonding chromium inside the grains. The formation of MC has been observed after short-term annealing at temperatures around 750°C. The temperature range of MC precipitation extends with increasing Ti and Nb bulk contents. The brittle σ-phase is a most common intermetalic phase precipitating in ASS.

Marshall examined several long-term serviced plant steels of the AISI 316 type and found $M_{23}C_6$ as the dominant phase; however traces of sigma phase, Laves phase and M_6C were also observed [7]. Terada in AISI 316L(N) did not found $M_{23}C_6$ after long time exposure [8]. Källqvist identified NbC and sigma phases in AISI 347 after exposure between 500 - 700°C for up to 70 000 hours [9]. $M_{23}C_6$ and sigma phases have been found in AISI 304 after annealing at 550 – 750°C for maximum 180 000 hours by Tanaka [10]. Erneman found in AISI 347 steel Nb(C,N), Z-phase, $M_{23}C_6$ and Cr_2N after long term exposure at 800°C. At 700°C, author distinguished between two types of Nb(C,N) and reported also about occurrence of R-phase [2].

The description of the phase evolution in ASS, marked as A, B, and C, during long term exposures at temperatures 600, 650 and 800°C is the main aim of this work. The approach combining experimental characterization with thermodynamic calculations by ThermoCalc was used in the investigation.

2 EXPERIMENTAL

The investigated steels (Table 1) were exploited in industry at 600, 650 and 800°C for long-terms (Table 2).

Table 1 Chemical compositions of austenitic stainless steels investigated [wt. %]

Steel	Alloying element									
	C	Mn	Si	Cr	Ni	Mo	Ti	Nb	S	P
A	0.06	1.67	0.62	18.48	8.37	0.30	-	-	0.025	0.030
B	0.10	1.59	0.74	17.71	9.32	0.52	-	0.56	0.026	0.030
C	0.12	0.6	1.00	21.02	30.07	0.25	0.45	-	0.005	0.030

The metallographic samples of the steels were prepared by standard procedures. After grinding they were polished using diamond pastes with the grain sizes of 6, 3 and 1 μm. Finally, the samples were etched either in 10% aqueous solution of oxalic acid or in Groesbeck (4g $KMnO_4$ + 4g NaOH + 100ml H_2O) that is agent used for the selective etching of carbides. The steel microstructure was observed by light microscopy. To identify secondary phase particles, scanning electron microscopy (SEM) and transmission electron microscopy (TEM) of thin foils and carbon extraction replicas were used. Thin foils were prepared by jet-electropolishing. Both selected area electron diffraction (SAED) and energy dispersive x-ray spectroscopy (EDX) were used to identify the particles.

3 THERMODYNAMIC CALCULATIONS

The Hillert-Staffason sublattice model was used for the modelling of secondary phase evolution [11]. The total Gibbs energy of the system consists of contributions of individual phases. Each of the phases considered is modelled as a sum of the reference level of Gibbs energy, entropy term, excess Gibbs energy, and magnetic term (if plausible the magnetic ordering). Besides phase equilibria, the chemical compositions and molar fractions of equilibrium phases were predicted. The Gibbs energies for bcc and fcc phases were described using the two-sublattice model consisting of metal and interstitial sublattices. The elements like Fe, Cr or Ni can substitute each other on the metal sublattice, and C and vacancies on the interstitial sublattice. For one formula unit (A, B, C)a(X, Va)c, the model gives:

$$\begin{aligned} G_m &= \sum_i y_i (y_X G^O_{i:X} + y_{Va} G^O_{i:Va}) + aRT \sum_i y_i \ln y_i + cRT (y_X \ln y_X + y_{Va} \ln y_{Va}) \\ &+ \sum_i \sum_j y_i y_j \left(y_X L_{i,j:X} + y_{Va} L_{i,j:Va} \right) + y_X y_{Va} \sum_i y_i L_{i:X,Va} \\ &+ \sum_i \sum_j \sum_k y_i y_j y_k \left(y_X L_{i,j,k:X} + y_{Va} L_{i,j,k:Va} \right) + G_{mag} \\ i &= A, B, C \text{ with } i \neq j, \text{ and } i \neq k, \text{ and } j \neq k, \end{aligned} \quad (1)$$

where y denotes the site fraction of component i in a sublattice. Symbols a and c denote the numbers of sites on each sublattice. In the case of bcc, a=1 and c=3, for fcc, a=c=1. $G^O_{i:Va}$ is the Gibbs energy of pure element i in a relevant non-magnetic state and $G^O_{i:X}$ is the Gibbs energy of a hypothetical non-magnetic state, where all interstitial sites are occupied by carbon. All values of G are given relative to the reference state which is defined as a standard state at 298.15 K and 105 Pa. L is the interaction parameter expressed by Redlich–Kister polynomial as a concentration dependence. G_{mag} is the magnetic part of the Gibbs energy [12].

The calculations have been made with the ThermoCalc software using the STEEL16F database formulated by Kroupa et al. [13]. The aim of the calculations consisted in prediction of phase equilibrium for various temperatures. All elements present in the investigated steels were considered except for sulphur and phosphorus (they are not included in the database). With respect to the literature, the following phases were considered in the calculations: liquid, austenite, ferrite, Laves, Sigma, $M_{23}C_6$, Chi, M_3C, M_6C, M_7C_3, and MC.

4 RESULTS

For steels A, B, and C, the typical microstructures are illustrated in Fig. 1 and average grain sizes are given in Table 2. Extremely large precipitates along the grain boundaries were observed in steel C (Fig.1d).

Table 2 Selected parameters characterizing the steels: exposure conditions, average grain sizes, and secondary phases identified

Steel	Temperature of exposure (°C)	Duration of exposure (year)	Average grain size in μm	Secondary phases identified (TEM, EDX)	
				Intergranular area	Intragranular area
A	600	3.5	65±27	$M_{23}C_6$ + Sigma	$M_{23}C_6$
B	650	10	20±5	$M_{23}C_6$ + Sigma	NbC
C	800	3	95±20	$M_{23}C_6$	TiC

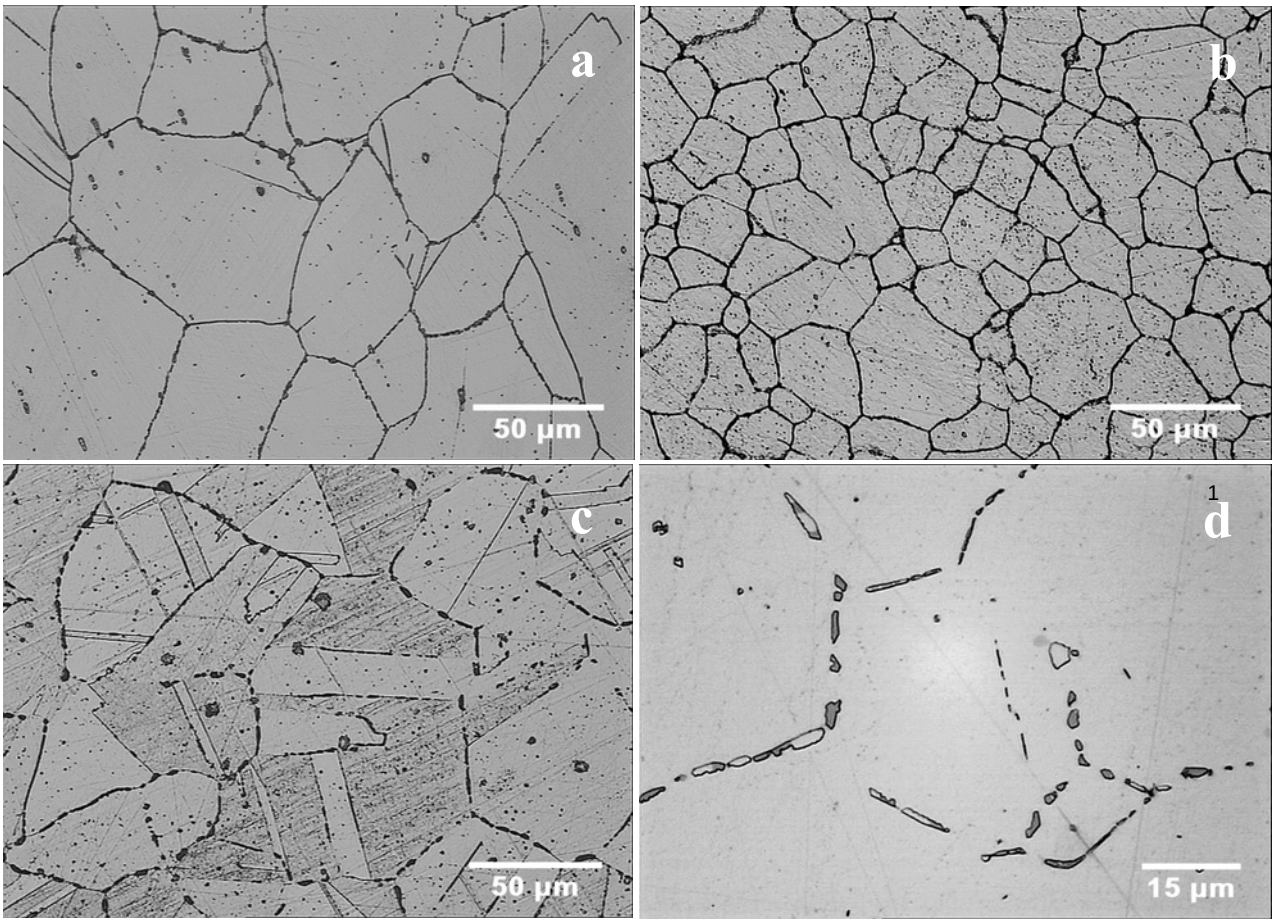

Figure 1 Microstructures of the steel A (a), B (b) and C (c) after etching in 10% aqueous solution of oxalic acid and morphology and distribution of large carbides in microstructure of the steel C (d) etched in Groesbeck (selective etchant for carbides), light microscopy

Particles of Sigma and $M_{23}C_6$ were found at the grain boundaries in steels A and B. Moreover, $M_{23}C_6$ was observed to precipitate inside the grains in steel A. In steel B, niobium-rich MC was identified in the grain interior next to the intergranular Sigma and $M_{23}C_6$. In steel C, MC was found to precipitate inside the grains and $M_{23}C_6$ mainly at the grain boundaries (Table 2).

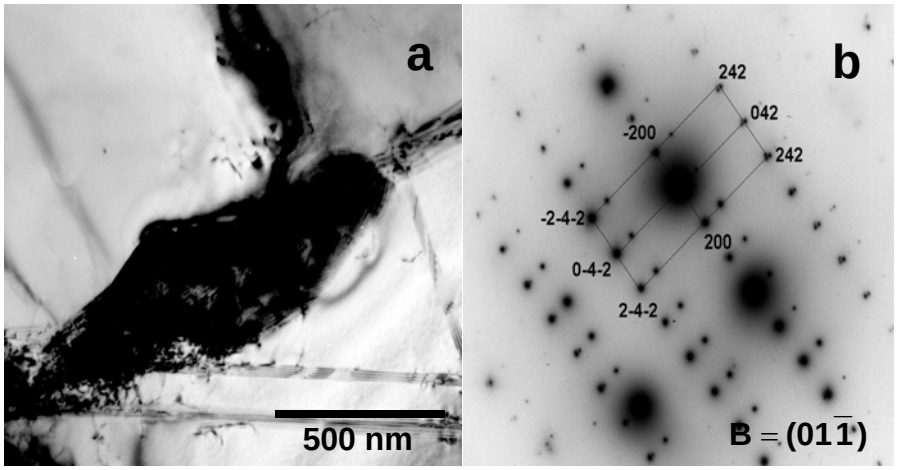

Figure 2 Particle of $M_{23}C_6$ identified in steel A (a) and the corresponding SAED pattern (b), TEM of thin foils

Thermodynamic calculations have been performed in the temperature range of 550-900°C (Table 3). According to the predictions, Sigma and $M_{23}C_6$ (600°C), $M_{23}C_6$ and MC (650°C), and MC (800°C) are stable phases for respective A, B, and C steels. Chemical compositions of $M_{23}C_6$ in steel C obtained by EDX and predicted by ThermoCalc are compared in Fig. 3. The calculated values correspond to 773°C, because this is the upper temperature limit of the $M_{23}C_6$ occurrence in equilibrium.

Table 3 Equilibrium phases predicted for systems corresponding to steels A, B, and C

Secondary phases predicted to be in equilibrium with austenite	Temperature range (°C)		
	Steel A	Steel B	Steel C
Sigma+MC+$M_{23}C_6$		550-656	
Sigma+$M_{23}C_6$	550-675		
MC+$M_{23}C_6$		657-878	550-773
$M_{23}C_6$	676-900		
MC		878-900	774-900

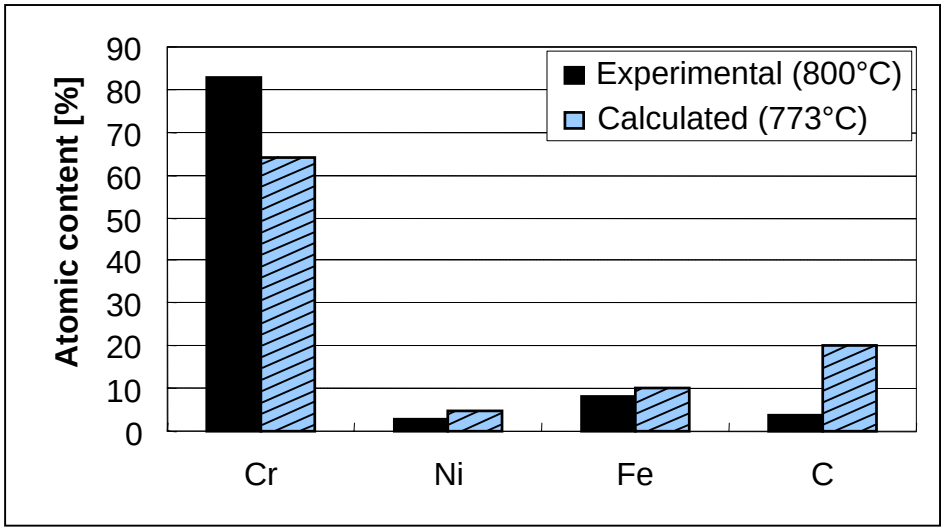

Figure 3 Comparison of experimentally determined and predicted atomic contents of Cr, Ni, Fe, and C in $M_{23}C_6$ for steel C. The predicted values correspond to 773°C

5 DISCUSSION

Microstructure of all studied steels consists of austenite and secondary phases in inter- and intra- granular positions. Steel A shows larger variance in grain sizes than two other steels (Fig. 1, Table 2), probably due to the pre-service heat treatment. It is probable that small particles of MC precipitated in steels B and C during the pre-service heat treatment done at about 1000°C.

In the steels, three types of secondary phases (Sigma, MC and $M_{23}C_6$) were identified after long-term service. With respect to the suggested heat treatment conditions, Sigma and $M_{23}C_6$ precipitated probably during the service, and MC started to precipitate already during the pre-service heat treatment [14, 15]. The formation of the Fe-Cr sigma phase [7] in steels A and B was driven by two factors. The first one resides in the higher Cr content, and rather low contents of Ni and C retarding the Sigma formation [16, 17]. The second factor applicable for steel B consists in the formation of carbon depletion zones around $M_{23}C_6$ particles due to the MC precipitation. The depletion zones seem to be ideal places for the Sigma formation. MC was found to precipitate within the grains (B and C steels) or in the form of carbide clusters at the grain boundaries. Janovec et al. [18] showed that the precipitation of Cr(Fe)-rich M_3C, M_7C_3 at the grain boundaries preceded the intergranular precipitation of V-rich MC in the 2.7Cr-0.6Mo-0.3V steel annealed at 720°C. If the mechanism described above is also applicable for the stabilized austenitic steels, $M_{23}C_6$ should to start precipitate earlier than MC

in steels B and C. Both the intergranular $M_{23}C_6$ and the intragranular MC particles are larger in steel C than in steel B (Fig. 1). It is probably a consequence of the higher service temperature of steel C. The size, quantity and distribution of MC particles are also dependent on the bulk concentration of stabilizing elements. Unfortunately, it is in both steels lower than recommended [19]. $M_{23}C_6$ was found to be the dominant precipitate in all the studied steels. The average length of intergranular particles in steel C exhibited about 4.000 nm, while the largest particles reached the length up to 10.000 nm.

Thermodynamic predictions of secondary phases for steels A and B showed full consistency with experimental results (Tables 2 and 3). In steel C, both $M_{23}C_6$ and MC were experimentally identified, but the only MC was predicted to be equilibrium phase co-existing with austenite at 800°C. This can be caused by several factors. For instance, steel C did not reach equilibrium at service conditions, or some factors stabilizing $M_{23}C_6$ were not taken into account in the calculations. The former factor is highly probable, because the maximum temperature of the $M_{23}C_6$ occurrence in equilibrium is 773°C and the equilibrium (calculated for 773°C) and experimentally determined contents of Cr, Fe, Ni, and C in $M_{23}C_6$ differ from each other (Fig. 3).

6 CONCLUSIONS

Various combinations of Sigma, MC and $M_{23}C_6$ phases were found in the investigated austenitic steels after long-term service at temperatures between 600 and 800°C. At the grain boundaries of steel C (21Cr-30Ni), large $M_{23}C_6$ particles (up to 10 μm in length) were identified even if this carbide was not predicted to be in equilibrium at 800°C. Otherwise, good agreement between the thermodynamically predicted (ThermoCalc) and experimentally achieved (TEM, EDX, SAED, SEM) results was stated.

Acknowledgment

The authors of the work wish to thank to the Grant Agency of the Ministry of Education and Slovak Academy of Sciences (VEGA) for financial support under the grant No. 1/0126/08.

References

[1] ANDERSSON, J-O, HELANDER, T., HÖGLUND, L., SHI P., SUNDMAN, B. Thermo-Calc & DICTRA, computational tools for materials science. *Calphad*, 2002,Vol. 26, No. 2, pp. 273-312

[2] ERNEMAN, J., SCHWIND, M., LIU, P., NILSSON, J. -O., ANDRÉN, H. -O., ÅGREN, J. Precipitation reactions caused by nitrogen uptake during service at high temperatures of a niobium stabilised austenitic stainless steel. *Acta Materialia,* 2004, 52, 4337-4350

[3] PADILHA, A. F., RIOS, P. R. Decomposition of austenite in austenitic stainless steels. *ISIJ Internacional*, 2002, 42, 325-337

[4] ZÁHUMENSKÝ, P., TULEJA, S., ORSZÁGHOVÁ, J., JANOVEC, J., MAGULA, V. Changes in corrosion resistance of 18%Cr-12%Ni-type stainless steels after sensitization. *Corrosion*, 57, 2001, 874-883

[5] PADILHA, A. F., ESCRIBA, D. M., MATERNA-MORRIS, E., RIETH, M., KLIMENKOV, M. Precipitation in AISI 316L(N) during creep tests at 550 and 600 °C up to 10 years. *Journal of Nuclear Materials,* 362*, 2007,* 132-138

[6] JESENSKÝ, M. *Structure stability and weldability of stainless steels. Doctoral Thesis*, MTF STU, Trnava, 2006.

[7] Marshall, P. *Austenitic stainless steels Microstructure and mechanical properties*. London, Elsevier, 1984, ISBN 0-85334-277-6

[8] TERADA, M., ESCRIBA,D.M., COSTA, I., MATERNA-MORRIS, E., PADILHA, A.F. Investigation on the intergranular corrosion resistance of the AISI 316L(N) stainless steel after long time creep testing at 600 °C. *Materials characterization*, in press, 2007.

[9] KÄLLQVIST, J., ANDRÉN, H.-O. Microanalysis of a stabilised austenitic stainless steel after long term ageing. *Materials Science and Engineering*, 1999, A270, 27–32

[10] TANAKA, H., MURATA, M., ABE, F., IRIE, H. Microstructural evolution and change in hardness in type 304H stainless steel during long-term creep. *Materials Science and Engineering*, 2001, A319*-321, 788-791

[11] KROUPA, A., VÝROSTKOVÁ, A., SVOBODA, M., JANOVEC, J. Carbide reactions and phase equilibria in low-alloy Cr-Mo-V steels tempered at 773-993 K. Part II: Theoretical calculations. *Acta Materialia,* 1998, Vol. 46., 39-49

[12] HOMOLOVÁ, V., JANOVEC, J., KROUPA, A. Experimental and thermodynamic studies of phase transformations in Cr-V low alloy steels. *Materials Science and Engineering,* 2002 A335,290–297

[13] KROUPA, A., HAVRÁNKOVÁ, J., COUFALOVÁ, M., SVOBODA, M., VŘEŠŤÁL, J. Phase diagram in the iron-rich corner of the Fe-Cr-Mo-V-C system below 1000 K. *Journal of Phase Equilibria,* 2001, 22 (3), 312-323

[14] ASM Handbook Volume 4: Heat Treating, ASM International, 1991, 1012, ISBN 978-0871703798

[15] STEFANESCU, D. M. ASM Handbook Volume 15: Casting, ASM International, 1988, 937, ISBN 978-0871700216

[16] PERRICONE, M.J., ANDERSON, T.D., ROBINO, C.V., DUPONT, J.N., MICHAEL, J.R. Effect of composition on the formation of sigma during single-pass welding of Mo-bearing stainless steels. *Metalurgical and Materials Transactions A*, 2007, 38, 1976-1990.

[17] SOURMAIL, T. Precipitation in creep resistant austenitic stainless steels. *Materials Science and Technology* 17 (1), 2001, pp. 1-14

[18] JANOVEC, J., MAGULA, V., HOLÝ, A. Influence of long-term isothermal exposures upon M7C3 carbide changes in 2.7Cr-0.6Mo-0.3V steel. *Kovové Materiály*, Vol. 30, 1992, 44-53

[19] BHADESHIA, H. K. D. H., SIR HONEYCOMBE, R. *Steels Microstructure and Properties*. Oxford: Third edition, 2006, ISBN 978-0-750-68084-4